Journal of Membrane Science 495 (2015) 439–444

Contents lists available at ScienceDirect

Journal of Membrane Science

journal homepage: www.elsevier.com/locate/memsci

Cross-linked graphene membrane for high-performance organics separation of emulsions

Guofeng Li [a], Xing Wang [a,*], Lei Tao [b], Yongsan Li [a], Kecheng Quan [a], Yen Wei [b], Lifeng Chi [c,d], Qipeng Yuan [a,**]

[a] The State Key Laboratory of Chemical Resource Engineering, Beijing University of Chemical Technology, Beijing 100029, PR China
[b] Department of Chemistry and The Tsinghua Center for Frontier Polymer Research, Tsinghua University, Beijing 100084, PR China
[c] Institute of Functional Nano & Soft Materials (FUNSOM), Soochow University, Suzhou 215123, PR China
[d] Physikalisches Institute, Münster University, Münster D-48149, Germany

ARTICLE INFO

Article history:
Received 14 May 2015
Received in revised form
24 July 2015
Accepted 23 August 2015
Available online 24 August 2015

Keywords:
Graphene membranes
Organics permeation
Cross-flow
Surface wettability
Cross-linkage

ABSTRACT

Recently, graphene oxide (GO) membranes are highly attractive for their exceptional separation performance. However, their sieving characteristics limit GO membranes for some important applications where organics are preferred or organic solvents are employed. In this work, a novel cross-linked graphene (CG) membrane is fabricated through compressing and then reducing a cross-linked GO aerogel. It achieved high-performance of organics separation with high flux (225 L m^{-2} h^{-1}) and purity (> 99.98%) even in a cross-flow separation model, where water was intercepted. Deep insight revealed that both the converted surface wettability and the remaining channels in the CG membrane were crucial for the high-performance of organics separation. Beyond that, this CG membrane offers many advantages, such as facile preparation, self-supporting, structural stability and adaptation in harsh acidic/basic/high-temperature conditions, demonstrating its great potential for practical applications.

1. Introduction

Graphene oxide (GO), a star nanomaterial in recent years [1–4], contains oxygenated functional groups on the unique two-dimensional and mono-atom thick graphene sheet, rendering it a good candidate for use in various fields, such as nanocomposites, energy-related materials, sensors, paper-like materials, field-effect transistors and biomedical applications [5–9]. Recently, GO membranes are highly attractive for their exceptional separation performance on treating gases, liquids and ions [10–21]. As a breakthrough, Geim's group found that water vapor can pass through a GO membrane as fast as no barrier, while some organic molecules are blocked [10]. Meanwhile, several studies have also demonstrated that GO membrane is an ideal pressure-driven filtration membrane [11,12], especially for water separation due to its high hydrophilicity and low friction for water molecules [13]. However, their sieving characteristics limit GO membranes for some important applications where organics are preferred or organic solvents are employed. For example, the separation of organic emulsions remains a global challenge for industry [22,23]. Energy-saving and high-performance membranes are highly desirable for this purpose.

For organics selective filtration, reduced GO (RGO), which is deoxygenated GO by thermal annealing [24] or chemical reduction [25], is suitable for the demand of interfacial hydrophobicity and lipophilicity. However, the interlayer spacing of RGO is known less than that of GO [26], resulting in blocking or unacceptable permeation flux [12]. For example, Nair's group recently reported that hydroiodic acid reduced GO membrane is a perfect barrier for blocking all gases, liquids and aggressive chemicals [27]. Considering that three-dimensional (3D) cross-linked graphene (CG) aerogel has porous structure and, especially, ultrafast oil absorbability [28], we suggest that using a cross-linked graphene oxide (CGO) membrane with post-reduction treatment can address the issues of organic emulsions separation.

With this strategy, the obtained CG membrane survived the chemical reduction while oxygen-related groups were removed. Both the needed channels within the cross-linked structure and the surface wettability were realized simultaneously. Herein, we present this novel CG membrane. It could achieve fast and selective permeation of organic solvents from various emulsions. Only tens to hundreds of ppm of water were detected in the organic filtrates. We demonstrated that besides the high-performance of organics separation, the designed CG membrane had basic advantages in aspects such as facile preparation, self-supporting, and

* Corresponding author. Fax: +86 1064416428.
** Corresponding author. Fax: +86 1064437610.
E-mail addresses: wangxing@mail.buct.edu.cn (X. Wang), yuanqp@mail.buct.edu.cn (Q. Yuan).

http://dx.doi.org/10.1016/j.memsci.2015.08.042
0376-7388/

structural stability, even countering the cross-flow separation used in industry [11,29,30].

2. Experimental section

2.1. Preparation of GO

Typically, 2 g graphite (80 mesh, purchased from Qingdao Jinrilai Co., Ltd., Shandong, China) and 1 g sodium nitrate were dispersed in 40 mL sulfuric acid (98%) at 0 °C. 6 g potassium permanganate was added and kept at 35 °C for 2 h. After adding 75 mL deionised water, the mixture was maintained at 98 °C for 15 min. Then, the mixture was diluted with 100 mL deionised water. 15 mL hydrogen peroxide (30%) was added gradually until the mixture turned yellow. After washing with water sufficiently, a GO solution (5 mg mL^{-1}) was obtained by ultrasonic exfoliation and centrifugation.

2.2. Preparation of CG membrane

Briefly, 1 mL ethylenediamine (EDA) and 100 mL GO solution (5 mg mL^{-1}) were sealed in a reactor (18 × 11 cm^2). After heating for 6 h at 95 °C, the CGO hydrogel was obtained with a size of 15 × 9 cm^2 [31]. Subsequently, the CGO aerogel was produced by freeze-drying treatment. After washing with ethanol sufficiently, the 3D-CGO aerogel was compressed to be a membrane at 6 MPa. This CGO membrane was reduced by a hydriodic acid solution (57%) at 95 °C for 10 min. After washing with ethanol sufficiently, the CG membrane was obtained. It can be tailored to a suitable shape and size for use in the separation apparatus (Supporting information, Scheme S1 and Fig. S1).

2.3. Membrane characterization

A HITACHI S4700 scanning electron microscopy (SEM) was used to image the unique characteristic of the CG membrane, as well as to perform the energy dispersive spectrometry (EDS) analysis. X-ray diffraction (XRD) patterns were recorded on a D/Max 2500 VB2+/PC in the range of 2θ=5–90°. Contact angle (CA) measurements were measured on a Dataphysics OCA20 at room temperature. De-ionized water and hexane (oil) were used here. Thermogravimetric analysis (TGA) was carried out with a Mettler Toledo TGA/DSC1/1100SF. Porosity was obtained by the Micromeritics ASAP 2020 Accelerated Surface Area and Porosimetry System V4.01. The N_2 volume was at standard temperature and pressure (STP). The P/P_0 represented the partial pressure of N_2 at equilibrium at 77 K. About 0.2 g of the samples was used in the test. The Derjaguin–Müller–Toporov (DMT) modulus was determined with a Bruker MultiMode 8 atomic force microscope (AFM). The values of the DMT modulus were determined at the corresponding vertical frequency values.

2.4. Preparation of emulsions

The emulsions were produced with a C25 emulsifying homogenizer (Shang Hai HENC Mechanical Equipment Co., Ltd.) at 16,000 rpm for 30 min. Surfactant-free emulsions were prepared from organic and water at a ratio of approximately 9:1. The emulsions of toluene, isooctane, petroleum ether, gasoline, diesel and soybean oil were termed from E-1 to E-6, respectively. Two surfactants, S-170 (RYOTO sugar esters) and LAS (linear-alkylbenzenesulfonic acid), were used in the preparation of surfactant-stabilised emulsions and strong acidic/basic emulsions. The compositions of the emulsions were shown in below: S-1 (toluene/water/S-170, 11.4 mL/100 μL/50 mg), S-2 (toluene/water/S-170, 5.8 mL/5.8 mL/50 mg), A-1 (toluene/HCl/LAS, 11.4 mL/100 μL/10 mg), B-1 (toluene/NaOH/LAS, 11.4 mL/100 μL/10 mg). 12 M HCl and NaOH solution were used here. The high-temperature emulsion was named T-1, which was composed of toluene (90%) and water (10%), mixed at 65 °C.

2.5. Separation of emulsions

A CG membrane was sealed between one vertical glass tube with a diameter of 15.5 mm and one sand-core filter plate (Fig. S2). The oil/water emulsions were poured onto the CG membrane and spontaneously permeated. The finally obtained organic filtrate was collected for purity tests. The flux was determined by calculating the permeated volume of the organic filtrate within 5 min.

For the cross-flow separation, the separation instrument was fabricated first. Briefly, a hatch (5 mm × 2 mm) was made on a hard tube. Then, the tube was partially attached by a sellotape with an aligned hatch. Finally, the hatch of the sellotape was covered by a piece of the CG membrane, and the CG membrane was grasped on the tube with the sellotape. When the separation instrument was generated, it was connected to a peristaltic pump with a soft silicone tube. The S-1 emulsion was continuously pumped into the instrument with a flow velocity of 5.5 L h^{-1}. Toluene permeated through the CG membrane and was collected for purity tests. The flux was determined by the above method.

3. Results and discussions

3.1. Characterization of the CG membrane

Fig. 1A shows that the thickness of the porous CGO aerogel

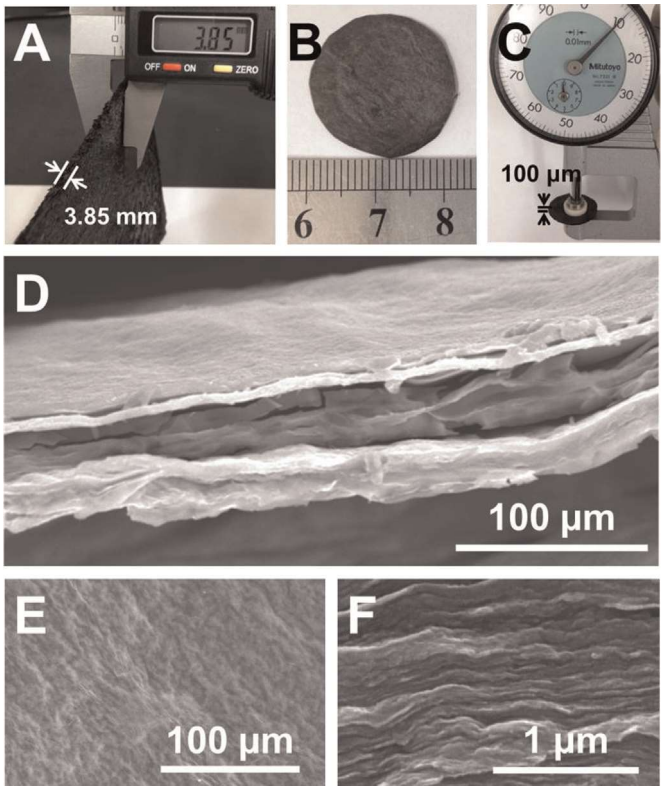

Fig. 1. The characterization of the CG membrane. (A) The thickness of the 3D CGO aerogel. (B) The tailored CG membrane. (C) The thickness of the CG membrane. (D) Cross-sectional SEM image of the CG membrane. A continuous thin surface layer could be found. (E) SEM image of the uniform membrane surface. (F) High-magnification SEM image of the stacked arrangement of cross-linked graphene sheets.

sponge is 3.85 mm. After compression and reduction, the final CG membrane can be tailored to a suitable shape and size (Fig. 1B). It should be emphasized that this CG membrane owns a dense-smooth and metallic luster surface. The thickness is approximately 100 μm (Fig. 1C). Scanning electron microscopy (SEM) shows that the CG membrane has a pronounced hierarchical layer structure (Fig. 1D) and uniform ripple-like surface (Fig. 1D and E). Although the tight stacking of graphene sheets is showed in the magnified cross-sectional image (Fig. 1F), the defects and opened spacing can be clearly observed in the middle layers of the CG membrane (Fig. 1D). The generation of the defects and spacing was mainly due to the following facts. Firstly, the original defects and spacing were produced in the formation process of the 3D-CGO aerogel. Then, the defects and spacing became smaller after compression. Finally, the sizes of the defects and spacing were further diminished because of the reduction treatment, in which the oxygen-related groups on the CGO membrane were removed.

The membrane's characteristic was first measured by energy dispersive spectrometry (EDS). Compared with that on the CGO membrane, the oxygen element detected on the CG membrane decreases from 11.1 wt% to 8.7 wt%, as shown in Fig. 2A, resulting in an increase of the C/O mole ratio from 7.0 to 9.4 after reduction treatment. X-ray diffraction (XRD) measurement further indicated this reduction process because the peak at 22.9° was weaker and a slight but distinct new peak emerged at 25.0° (Supporting information, Fig. S3). This result is consistent with the previous study that GO reduction generally leads to a relatively higher 2θ [26].

One of the important contributions of the reduction treatment on the CGO membrane is the change of wettability [27], which is considered to be a critical factor to the oil/water separation performance [23]. Thus, dynamic contact angle (CA) was used to test the changes. On the CGO membrane surface, the water CA changes from the initial 45° to 0° within 1.25 s (blue solid triangles in Fig. 2B), while the oil CA decreases from 10° to 0° within 1 s (blue hollow triangles in Fig. 2B). These phenomena indicated that the EDA linkers did not change the amphiphilic nature of GO nanosheets. However, after the treatment of the post-reduction, the CG membrane becomes hydrophobic and lipophilic. As shown in the right inset images of Fig. 2B, the oil (hexane) can be ultrafast adsorbed in the CG membrane only within 200 ms (also see red diamond in Fig. 2B), much faster than that of the CGO membrane (~1 s). On the other hand, a water droplet can stably stand on the CG membrane surface (red square in Fig. 2B). Only water evaporation can be recorded because the change of water CA is just like on the silicon wafer (black round in Fig. 2B). Therefore, the surface hydrophobicity and lipophilicity are essential for allowing oil but resisting water to pass through the CG membrane.

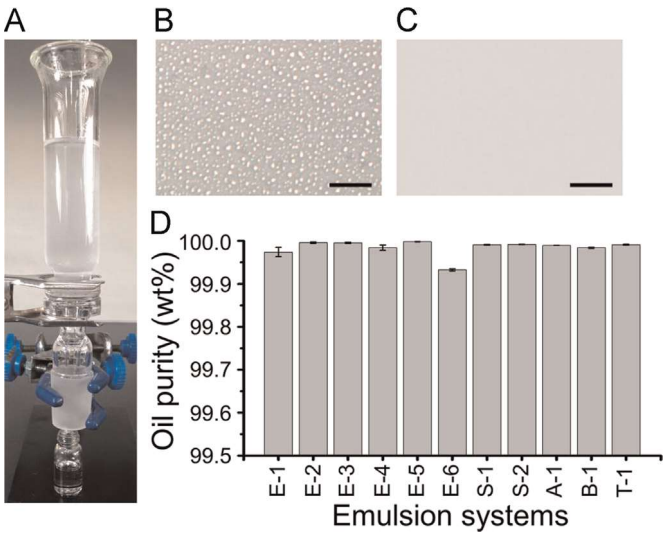

Fig. 3. Emulsions separation process and efficiency. (A) Photograph of a white emulsion separation, where oil selectively permeates through the CG membrane. (B) and (C) show the typical emulsion, S-1, before and after filtration. Scale bar: 5 μm. (D) Oil purity of filtrates after separation for various emulsion systems: E-1 (toluene/water, 9:1), E-2 (isooctane/water, 9:1), E-3 (petroleum ether/water, 9:1), E-4 (gasoline/water, 9:1), E-5 (diesel/water, 9:1), E-6 (soybean oil/water, 9:1), S-1 (toluene/water/S-170, 11.4 mL/100 μL/50 mg), S-2 (toluene/water/S-170, 5.8 mL/5.8 mL/50 mg), A-1 (toluene/HCl/LAS, 11.4 mL/100 μL/10 mg), B-1 (toluene/NaOH/LAS, 11.4 mL/100 μL/10 mg), and T-1 (toluene/water, 9:1, 65 °C). Every group of the separation was performed at least 4 times.

3.2. The CG membrane performance for organics separation

We initially separated toluene–water emulsion (E-1, initial ratio v/v=9:1) with our tailored CG membrane. Under ambient condition as shown in Fig. 3A, toluene spontaneously permeates through the CG membrane with a high flux (approximately 212 L m^{-2} h^{-1}) in the apparatus, where gravity is the driving force for the separation. The purity of the toluene filtrate is up to 99.98 wt%, as evaluated by a Karl Fischer analyzer. Only 154 ppm of water, even better than the commercial standard (≤200 ppm, Sigma-Aldrich®), was detected in the toluene filtrate. Then, we tested other emulsion systems (E-2 and E-3 in Fig. 3D and Table S1 in Supporting information). Remarkably, for the separation of normal organic solvents such as isooctane/water (E-2) and petroleum ether/water (E-3) mixtures (v/v=9:1), only ~17 ppm (the commercial standard of isooctane is ≤30 ppm, Sigma-Aldrich®)

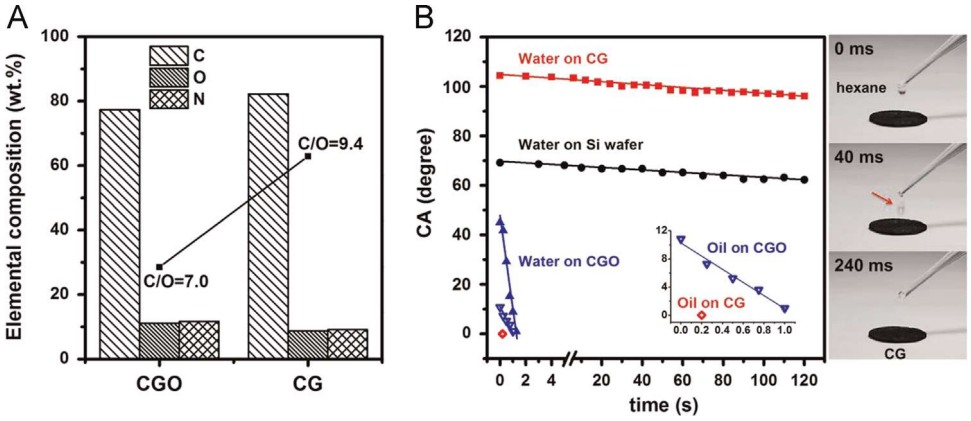

Fig. 2. Surface properties of the CG and CGO membranes. (A) EDS characterization of the CG and CGO membranes. (B) Dynamic contact angle (CA) measurements of the CG and CGO membranes. The insets show the ultrafast adsorbing of hexane in a CG membrane within 200 ms. (For interpretation of the references to color in this figure, the reader is referred to the web version of this article.)

and ~26 ppm (the commercial standard of petroleum ether is ≤50 ppm, Sigma-Aldrich®) of water were detected, respectively. These performances demonstrated a promising prospect of the CG membrane for use in the field of refining organics.

Further detections were carried out with emulsions on the basis of gasoline (E-4), diesel (E-5) and soybean oil (E-6) because they are widely used in our lifeway. As a result, the filtrates of E-4 and E-5 displayed trace water as little as ~108 ppm and ~18 ppm (≤200 ppm, EU standard EN 590) [32], respectively. The filtrate purity of E-6 is 99.93 wt%, and its quality has been eminently satisfactory for the food processing industry, as the standard is >99.80 wt% (GB1535-2003, China).

Separation of surfactant-stabilized emulsion is generally considered to be challenging. Hence, we used two surfactants, S-170 (RYOTO sugar esters) and LAS (linear-alkylbenzenesulfonic acid), to investigate the separation performance of the CG membrane. The S-170 was used in toluene/water emulsions, in which the water droplets in the emulsions were very small (diameter of approximately 0.2–0.6 μm, as shown in Fig. 3B). After separating with the CG membrane, clear organic filtrates were received (Fig. 3C), and the water content in the filtrates was below 100 ppm (84 ppm in S-1 and 78 ppm in S-2). The recovery ratio of the toluene was around 70% due to the enrichment of the water droplets with the S-170. Most of the S-170 was retained in the remained solution as its concentration in the remained solution rose to 1.7 mg mL^{-1} from 0.6 mg mL^{-1} of the original emulsion. Besides, the LAS was used in a strong acidic emulsion (A-1) and a strong basic emulsion (B-1). Under those harsh acidic/basic conditions, the organic filtrates displayed a distinct pH change to neutral (Supporting information, Fig. S4). The water content in the A-1 and in the B-1 was 103 ppm and 152 ppm, respectively.

In addition, the CG membrane exhibits a good performance under high temperatures (65 °C) as shown in Fig. 2D (T-1, also see Fig. S5 in Supporting information). This performance was supported by the thermogravimetric analysis (TGA), in which the CG membrane was thermal stability until near 300 °C (Supporting information, Fig. S6).

3.3. The pathways of organic molecules permeating through the CG membranes

The defects and the spacing between the cross-linked graphene nanosheets are important pathways for organic molecules permeating through the CG membrane. Peng's group recently found that nanochannels within the GO membranes are mainly composed of inter-spacing, wrinkles and the nanopores caused by structural defects [33]. The pores will shorten the channel length so that the organic molecules permeate through the membrane easily. As mentioned above, it was no doubt that there were many porous structures in the original CGO membrane, and those porous structures would remain to a certain degree in the CG membrane.

Therefore, N_2 adsorption–desorption isotherms were used to analyze the pores of the membranes as shown in Fig. 4A. According to the IUPAC classification, the N_2 adsorption–desorption isotherms of the CGO and the CG membrane are assigned to type IV with H3 hysteresis loop in the P/P_0 range of 0.45–0.95 [34]. It suggests that the CGO and the CG membrane are lamellar-stacked structures. BJH pore size distributions analysis (Fig. 4B) shows that the original CGO membrane has a broad peak for the adsorption pore diameter, ranging from 6.0 nm to 110.6 nm. The adsorption average pore diameter is 10.1 nm. Compared with that of the CGO membrane, the pore diameter of the CG membrane decreases distinctly. The peak of the adsorption pore diameter mainly ranges from 3.3 nm to 40.1 nm, and the adsorption average pore diameter is 7.0 nm. These results indicated that the pores of the CG membrane shrunk because of the reduction treatment of hydriodic acid. In addition, the CG membrane exhibits a new peak for the adsorption average pore diameter at 1.9 nm, which is corresponding to the spacing between the restacked cross-linked graphene nanosheets. Because the reduction treatment removed the oxygen-related groups, the spacing of the CG membrane decreased so that the peak at 1.9 nm became apparent. Huang et al. [12] reported that GO membrane owns the spacing in the range of 0.6–1.0 nm depending on the different fabrication methods. Herein, the EDA linkers created wider spaces approximately 1.9 nm that is in agreement with the previous investigation [35].

3.4. Effect of reduction time and membrane thickness on the separation performance

The reduction process has an important effect on the separation performance of the CG membrane. Fig. 5A shows the plot of reduction time ranging from 1 min to 30 min versus flux by using the CG membrane with a thickness of approximately 80 μm. The flux is up to 411 L m^{-2} h^{-1} after 1 min reduction treatment. However, the filtrate was cloudy. Water could not be separated from the oil/water emulsion because the membrane was not reduced sufficiently. Until the reduction treatment increased to 5 min, the filtrate was clear. But with prolonging the reduction time, the flux decreases. This decreasing flux was mainly caused by the change of pore structure on the CG membrane surface. As mentioned above, the reduction treatment shrunk the pore of the CG membrane. With the reduction time extending, more and more oxygen-containing functional groups were remove. The spacing decreased, thus the CG membrane surface became tightly. As a

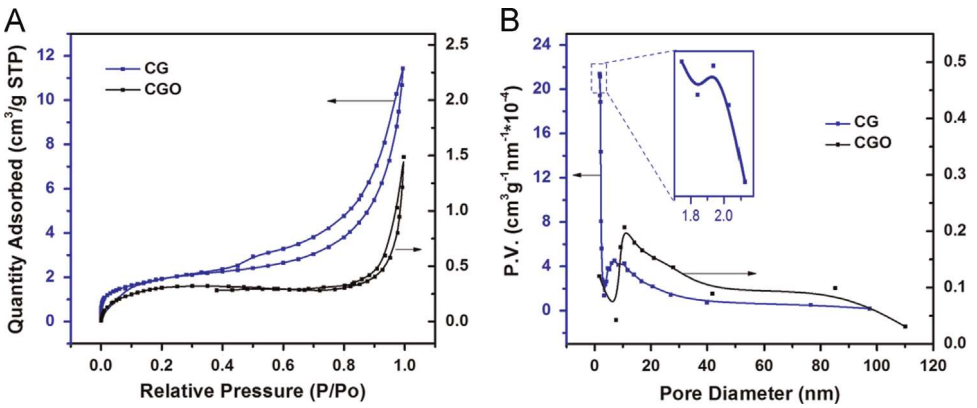

Fig. 4. The pore distributions of the CG and CGO membranes were analyzed by a Micromeritics ASAP 2020. (A) N_2 adsorption–desorption isotherms. (B) BJH pore size distributions based on N_2 adsorption–desorption isotherms. "P.V." is short for "Pore Volume".

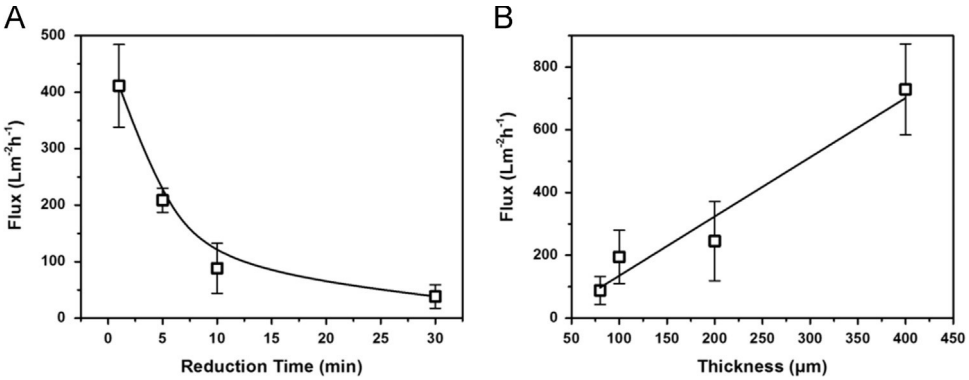

Fig. 5. Effect of the reduction time (A) and the membrane thickness (B) on the CG membrane flux. The toluene/water emulsion (E-1) was used. Every data points were performed 4 times.

result, the flux decreased with the increase of the reduction time.

The membrane thickness is another influencing factor. Previous study showed that thinner thickness of the membrane contributed to the ultrafast separation [36]. Hence, we modulated the volume of the GO suspension in the fixed container to obtain the CG membranes with different thicknesses. The reduction time was fixed at the same 10 min for all the membranes. However, different from our expectation, the flux is 88 L m^{-2} h^{-1} when the thickness of the CG membrane is approximately 80 μm, while the flux increases up to 729 L m^{-2} h^{-1} when the thickness increases to approximately 400 μm (Fig. 5B). These phenomena suggested that with the increase of the membrane thickness, the flux becomes gradually higher. We speculated that one possible reason might be the freeze-drying process within the fabrication. As reported, O'Brien et al. [37] studied the effect of freeze-drying on the pore structure of the material. They found that the mean pore size of the material produced using smaller pan is significantly smaller ($p < 0.05$) than that of the material produced using larger pan. Therefore, freeze-drying might produce more defects and pores in the thick aerogel than in the thin one. Both the defects and the pores were remained to a certain degree in the CG membranes even after being compressed and reduced. As evidence, we found that with the increase of the membrane thickness, water content in the oil filtrate increased (Table S2). This result suggested that the pore size of the CG membrane increased within thicker CG membrane. In addition, the consumption of the reduction agent in the thick CG membrane was higher than that in the thin one so that the reduction agent acted on the surface of the thick CG membrane may be cut back. Therefore, the reduction layer on the thick membrane surface became thinner, leading to the increase of the flux. As mentioned above, the generation of the pore structure would affect the oil/water separation performance. Increasing the thickness of the CG membrane was in favors of enhancing the flux of organics, whilst scarifying the organic purity. Based on aforementioned results, 100-μm-thick CG membrane with 10 min reduction treatment was suitable for high-flux organics separation. This CG membrane finally achieved high fluxes on the order of 10^2 L m^{-2} h^{-1} for many organics separation (Supporting information, Table S3) under ambient pressure.

3.5. *Cross-flow separation performance*

Cross-flow separation technology has been used widely in industry globally owning to its advantages such as continuous operation, energy saving and high-performance. However, the tangential motion of the bulk of fluids will cause fluid friction on the membrane surface, demanding sufficient stability of the membrane. Whereas laminar GO membranes assembled with GO sheets currently could not overcome this formidable challenge. As this CG membrane was reduced from the cross-linked structure, the mechanical strength increased on the surface [26,38]. Nanoindentation measurements showed that the Derjaguin–Müller–Toporov (DMT) modulus of the CG (~12 GPa) was three times higher than that of the CGO (~4 GPa), indicating a sufficient structural strength of the CG membrane (Supporting information, Fig. S7). Considered that this internal cross-linked architecture had more distinct advantage than the laminar GO membranes, a cross-flow separation apparatus was constructed (Fig. 6). The CG membrane is self-standing on a 5 mm × 2 mm hatch in the apparatus, withstanding the pressure of the fluid. The toluene filtrate was obtained with flux of approximately 225 L m^{-2} h^{-1} and purity of 99.98 wt%, demonstrating the remarkable performance of the CG membrane for cross-flow separation. Moreover, our recent study showed that the CG membrane used in a mini practical cross-flow device achieved good separation performance as well as the above-mentioned apparatus. Therefore, the CG membrane displayed great potential for cross-flow separation application in industry. It will be further studied in our following works.

4. Conclusion

Oil/water separation has been a worldwide subject. Polymer membranes were usually served as commercial products in this field because of their excellent manufacture and performance [39,40]. However, polymer membranes are still limited under some harsh conditions. Therefore, scientists recently pay more attention on graphene-based membranes due to their more structural and chemical stability. Super-performances were realized on many graphene-based membranes, especially for water separation of various oil/water mixtures and emulsions [19]. But

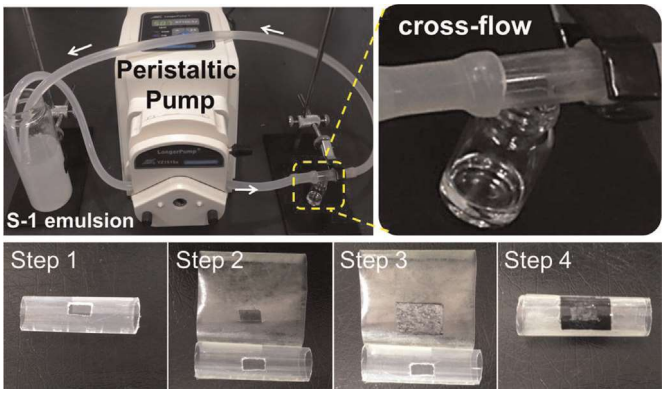

Fig. 6. A cross-flow separation instrument fitted with our CG membrane. The inset shows the fabrication process. See details in Section 2.5.

still few studies reported organics separation and demonstrated good performances. This novel CG membrane achieved high-performance of organics separation with high purity (> 99.98%) and flux (225 L m^{-2} h^{-1}), which is close to that of the commercial polymer-based ultrafiltration membrane (usually with a flux of less than 300 L m^{-2} h^{-1}) [40]. Thus, this CG membrane can be a competing candidate for organics separation.

In summary, producing a CG membrane from a CGO aerogel not only supplied a facile method to create a useful graphene-based membrane, but also demonstrated high performance for organics separation, especially in terms of separation efficiency including the ideal filtrate purity and fast flux. Besides that, many advantages such as self-supporting, modularity, structural stability and adaptation under harsh acidic/basic/high-temperature conditions were also demonstrated. Furthermore, a superior characteristic should be noted that this CG membrane could be used in a cross-flow separator with the same high-performance, thus demonstrating great potential for practical applications in industry.

Notes

The authors declare no competing financial interest.

Acknowledgment

The authors thank the National Natural Science Foundation of China (21204004, 21376017), Beijing Natural Science Foundation (2132040), Specialized Research Fund for the Doctoral Program of Higher Education (20120010120011), and Fundamental Research Funds for Central Universities (YS1407) of China for funding support.

Appendix A. Supplementary material

Supplementary data associated with this article can be found in the online version at http://dx.doi.org/10.1016/j.memsci.2015.08.042.

References

[1] A.K. Geim, K.S. Novoselov, The rise of graphene, Nat. Mater. 6 (2007) 183–191.
[2] D.R. Dreyer, S. Park, C.W. Bielawski, R.S. Ruoff, The chemistry of graphene oxide, Chem. Soc. Rev. 39 (2010) 228–240.
[3] D. Chen, H. Feng, J. Li, Graphene oxide: preparation, functionalization, and electrochemical applications, Chem. Rev. 112 (2012) 6027–6053.
[4] V. Georgakilas, M. Otyepka, A.B. Bourlinos, V. Chandra, N. Kim, K.C. Kemp, P. Hobza, R. Zboril, K.S. Kim, Functionalization of graphene: covalent and non-covalent approaches, derivatives and applications, Chem. Rev. 112 (2012) 6156–6214.
[5] X. Huang, X. Qi, F. Boey, H. Zhang, Graphene-based composites, Chem. Soc. Rev. 41 (2012) 666–686.
[6] Y. Li, Y. Hu, Y. Zhao, G. Shi, L. Deng, Y. Hou, L. Qu, An electrochemical avenue to green-luminescent graphene quantum dots as potential electron-acceptors for photovoltaics, Adv. Mater. 23 (2011) 776–780.
[7] D. Li, M.B. Müller, S. Gilje, R.B. Kaner, G.G. Wallace, Processable aqueous dispersions of graphene nanosheets, Nat. Nanotechnol. 3 (2008) 101–105.
[8] V.C. Tung, M.J. Allen, Y. Yang, R.B. Kaner, High-throughput solution processing of large-scale graphene, Nat. Nanotechnol. 4 (2008) 25–29.
[9] S. Yin, Y. Goldovsky, M. Herzberg, L. Liu, H. Sun, Y. Zhang, F. Meng, X. Cao, D. D. Sun, H. Chen, A. Kushmaro, X. Chen, Functional free-standing graphene honeycomb films, Adv. Funct. Mater. 23 (2013) 2972–2978.
[10] R.R. Nair, H.A. Wu, P.N. Jayaram, I.V. Grigorieva, A.K. Geim, Unimpeded permeation of water through helium-leak-tight graphene-based membranes, Science 335 (2012) 442–444.
[11] H. Huang, Y. Ying, X. Peng, Graphene oxide nanosheet: an emerging star material for novel separation membranes, J. Mater. Chem. A 2 (2014) 13772–13782.
[12] K. Huang, G. Liu, Y. Lou, Z. Dong, J. Shen, W. Jin, A graphene oxide membrane with highly selective molecular separation of aqueous organic solution, Angew. Chem. Int. Ed. 53 (2014) 6929–6932.
[13] R. Liu, G. Arabale, J. Kim, K. Sun, Y. Lee, C. Ryu, C. Lee, Graphene oxide membrane for liquid phase organic molecular separation, Carbon 77 (2014) 933–938.
[14] H. Li, Z. Song, X. Zhang, Y. Huang, S. Li, Y. Mao, H.J. Ploehn, Y. Bao, M. Yu, Ultrathin, molecular-sieving graphene oxide membranes for selective hydrogen separation, Science 342 (2013) 95–98.
[15] L. Qiu, X. Zhang, W. Yang, Y. Wang, G.P. Simon, D. Li, Controllable corrugation of chemically converted graphene sheets in water and potential application for nanofiltration, Chem. Commun. 47 (2011) 5810–5812.
[16] Y. Han, Z. Xu, C. Gao, Ultrathin graphene nanofiltration membrane for water purification, Adv. Funct. Mater. 23 (2013) 3693–3700.
[17] R.K. Joshi, P. Carbone, F.C. Wang, V.G. Kravets, Y. Su, I.V. Grigorieva, H.A. Wu, A. K. Geim, R.R. Nair, Precise and ultrafast molecular sieving through graphene oxide membranes, Science 343 (2014) 752–754.
[18] H. Huang, Y. Mao, Y. Ying, Y. Liu, L. Sun, X. Peng, Salt concentration, pH and pressure controlled separation of small molecules through lamellar graphene oxide membranes, Chem. Commun. 49 (2013) 5963–5965.
[19] X. Hu, Y. Yu, J. Zhou, Y. Wang, J. Liang, X. Zhang, Q. Chuang, L. Song, The improved oil/water separation performance of graphene oxide modified Al_2O_3 microfiltration membrane, J. Membr. Sci. 476 (2015) 200–204.
[20] H. Wu, B. Tang, P. Wu, Development of novel SiO_2–GO nanohybrid/polysulfone membrane with enhanced performance, J. Membr. Sci. 451 (2014) 94–102.
[21] J. Lee, H. Chae, Y.J. Won, K. Lee, C.H. Lee, H.H. Lee, I.C. Kim, J.M. Lee, Graphene oxide nanoplatelets composite membrane with hydrophilic and antifouling properties for wastewater treatment, J. Membr. Sci. 448 (2013) 223–230.
[22] M.A. Shannon, P.W. Bohn, M. Elimelech, J.G. Georgiadis, B.J. Marinas, A. M. Mayes, Science and technology for water purification in the coming decades, Nature 452 (2008) 301–310.
[23] Z. Xue, Y. Cao, N. Liu, L. Feng, L. Jiang, Special wettable materials for oil/water separation, J. Mater. Chem. 2 (2014) 2445–2460.
[24] H.A. Becerril, J. Mao, Z. Liu, R.M. Stoltenberg, Z. Bao, Y. Chen, Evaluation of solution-processed reduced graphene oxide films as transparent conductors, ACS Nano 2 (2008) 463–470.
[25] H.J. Shin, K.K. Kim, A. Benayad, S.M. Yoon, H.K. Park, I.S. Jung, M. Jin, H.K. Jeong, J.M. Kim, J.Y. Choi, Y.H. Lee, Efficient reduction of graphite oxide by sodium borohydride and its effect on electrical conductance, Adv. Funct. Mater. 19 (2009) 1987–1992.
[26] S. Pei, J. Zhao, J. Du, W. Ren, H. Cheng, Direct reduction of graphene oxide films into highly conductive and flexible graphene films by hydrohalic acids, Carbon 48 (2010) 4466–4474.
[27] Y. Su, V.G. Kravets, S.L. Wong, J. Waters, A.K. Geim, R.R. Nair, Impermeable barrier films and protective coatings based on reduced graphene oxide, Nat. Commun. 5 (2014) 4843.
[28] T. Wu, M. Chen, L. Zhang, X. Xu, Y. Liu, J. Yan, W. Wang, J. Gao, Three-dimensional graphene-based aerogels prepared by a self-assembly process and its excellent catalytic and absorbing performance, J. Mater. Chem. A 1 (2013) 7612–7621.
[29] C. Cheng, D. Li, Solvated graphenes: an emerging class of functional soft materials, Adv. Mater. 25 (2013) 13–30.
[30] D.R. Paul, Creating new types of carbon-based membranes, Science 335 (2012) 413–414.
[31] H. Hu, Z. Zhao, W. Wan, Y. Gogotsi, J. Qiu, Ultralight and highly compressible graphene aerogels, Adv. Mater. 25 (2013) 2219–2223.
[32] J. Krahl, G. Knothe, A. Munack, Y. Ruschel, O. Schröder, E. Hallier, G. Westphal, J. Bünger, Comparison of exhaust emissions and their mutagenicity from the combustion of biodiesel, vegetable oil, gas-to-liquid and petrodiesel fuels, Fuel 88 (2009) 1064–1069.
[33] H. Huang, Z. Song, N. Wei, L. Shi, Y. Mao, Y. Ying, L. Sun, Z. Xu, X. Peng, Ultrafast viscous water flow through nanostrand-channelled graphene oxide membranes, Nat. Commun. 4 (2013) 2979.
[34] B. Shen, D. Lu, W. Zhai, W. Zheng, Synthesis of graphene by low-temperature exfoliation and reduction of graphite oxide under ambient atmosphere, J. Mater. Chem. C 1 (2013) 50–53.
[35] C. Song, T. Kwon, J.H. Han, M. Shandell, M.S. Strano, Controllable synthesis of single-walled carbon nanotube framework membranes and capsules, Nano Lett. 9 (2009) 4279–4284.
[36] Z. Shi, W. Zhang, F. Zhang, X. Liu, D. Wang, J. Jin, L. Jiang, Ultrafast separation of emulsified oil/water mixtures by ultrathin free-standing single-walled carbon nanotube network films, Adv. Mater. 25 (2013) 2422–2427.
[37] F.J. O'Brien, B.A. Harley, I.V. Yannas, L.J. Gibson, Influence of freezing rate on pore structure in freeze-dried collagen-GAG scaffolds, Biomaterials 25 (2004) 1077–1086.
[38] H. Chen, M.B. Müller, K.J. Gilmore, G.G. Wallace, D. Li, Mechanically strong, electrically conductive, and biocompatible graphene paper, Adv. Mater. 20 (2008) 3557–3561.
[39] W. Zhang, Z. Shi, F. Zhang, X. Liu, J. Jin, L. Jiang, Superhydrophobic and superoleophilic PVDF membranes for effective separation of water-in-oil emulsions with high flux, Adv. Mater. 25 (2013) 2071–2076.
[40] M. Huang, Y. Si, X. Tang, Z. Zhu, B. Ding, L. Liu, G. Zheng, W. Luo, J. Yu, Gravity driven separation of emulsified oil-water mixtures utilizing in situ polymerized superhydrophobic and superoleophilic nanofibrous membranes, J. Mater. Chem. A 1 (2013) 14071–14074.